

Enhancing the Life Cycle Performance of Gel Lead Acid Batteries Various Temperature Curing Algorithms on the Positive Plate

Dr. James Mark Stevenson¹, Kalyana Sundaram. G², Sakthivel Murugaiyan³, KD Merz⁴, Ajay Sharma⁵, Neelakkanan Rangaswamy⁶, Srinivasan Iyyappan⁷, Muthukumarasamy⁸, Revanth Durai⁹, Shivam Tiwari¹⁰, Gurunathan Manoharan¹¹

^{1, 2, 3, 5, 6, 7, 8, 9, 10, 11} Eternity Technologies FZ - LLC, Al Hamra Industrial Zone, Al Jazeera, Al Hamra, PO Box 35102, Ras Al Khaimah, UAE

⁴Abertax® Technologies Ltd. KW17A, Corradino Industrial Estate, PLA3000, Paola, Malta

Corresponding Author: *mark.stevenson[at]eternitytechnologies.com*,
kalyan.sundar[at]eternitytechnologies.com
Sakthivel.Murugaiyan[at]eadl.ae
kdmerz[at]online.de
ajay.sharma[at]eternitytechnologies.com
neela.kkanan[at]eternitytechnologies.com
srinivasan.iyyappan[at]eternitytechnologies.com
muthu.kumar[at]eternitytechnologies.com
revanth.durai[at]eternitytechnologies.com
shivam.tiwari[at]eadl.ae
gurunathan[at]eternitytechnologies.com

Abstract: *The lead - acid battery is preferred for energy storage applications due to its operational safety and low cost. However, the cycling performance of the positive electrode is significantly compromised by fast capacity decay caused by the softening and shedding of positive active material (PAM). The curing process imparts a crystalline structure to the active material, acting as a skeleton for the micro - crystalline structures established during formation. This article reports on high - and low - temperature curing algorithms for positive plates used in valve - regulated gel batteries for a 70% depth of discharge (DOD) performance test. The high - temperature - cured plate exhibited a 4BS crystal for cyclic performance, while the low - temperature - cured plate had a 3BS crystal for high initial capacity and cranking applications. Our experimental results show that the higher - temperature curing algorithm yields better 70% DOD performance than the low - temperature curing algorithm.*

Keywords: Lead Acid Batteries, Active Material, Silica Gel Batteries, Curing Profile, Life Cycle, Capacity Performance, Curing Chamber, Paste Mixing

Glossary and Nomenclature

AGM: Absorbed Glass Mat
AM: Active Material
VRLA: Valve - Regulated Lead Acid
LAB: Lead Acid Batteries
R&D: Research and Development
XRD: X - Ray Diffraction
SEM: Scanning Electron Microscopy
DM: De Mineralized
3BS: Tri Basic Lead Sulphate
4BS: Tetra Basic Lead Sulphate
NAM: Negative Active Material
PAM: Positive Active Material
CHA: Charge
DCH: Discharge
PAU: Pause
IEC: International Electrochemical Commission
DOD: Depth of Discharge
CC: Constant Current
CV: Constant Voltage
BFD: Before Flash Dryer
AFD: After Flash Dryer

RL: Residual Lead

LTCP: Low - Temperature Curing Profile

HTCP: High - Temperature Curing Profile

CN: Nominal Capacity

1. Introduction

In the field of lead - acid batteries, the curing process held immense significance in achieving efficient battery performance. Manufacturers universally adopted two curing methods: low - temperature curing and high - temperature curing [1]. Curing involves the formation of a corrosion layer between the active material and grids through the oxidation of free lead by oxygen present in a chamber under elevated humidity conditions, irrespective of temperature algorithm. Generally, low - temperature curing provided favorable battery capacity and performance at higher discharge rates. The prevailing phase in low - temperature curing was 3BS, depending on the chemical composition of the paste mix. Some industrial applications favored 4BS crystal formation during curing, as it enhanced cycle life in deeper discharge scenarios [2]. Certain studies even proposed incorporating 4BS crystals directly into the paste mix, generating smaller

Volume 13 Issue 4, April 2024

Fully Refereed | Open Access | Double Blind Peer Reviewed Journal

www.ijsr.net

4BS crystals. This aided in achieving the required level of positive active materials after the formation process, particularly for low Ah/Kg input during formation.

This study aimed to compare the influence of low - temperature and high - temperature curing profiles on the life cycle performance of industrial gel batteries [3]. The curing reaction established a foundational skeleton layer, which subsequently developed further during the post - formation process. The initial skeleton formation was achieved through controlled curing temperatures and humidity levels, dependent on moisture content and residual lead presence during paste mixing.

In this study, corrosion layer thickness was measured after curing in both low - temperature and high - temperature curing programs. Additionally, physical assessments were conducted to verify the adhesion and cohesion between paste and grids.

Curing Reaction:

Throughout the curing process, paste particles link together, creating a continuous and robust porous structure (skeleton) that is firmly adhered to the grid [4]

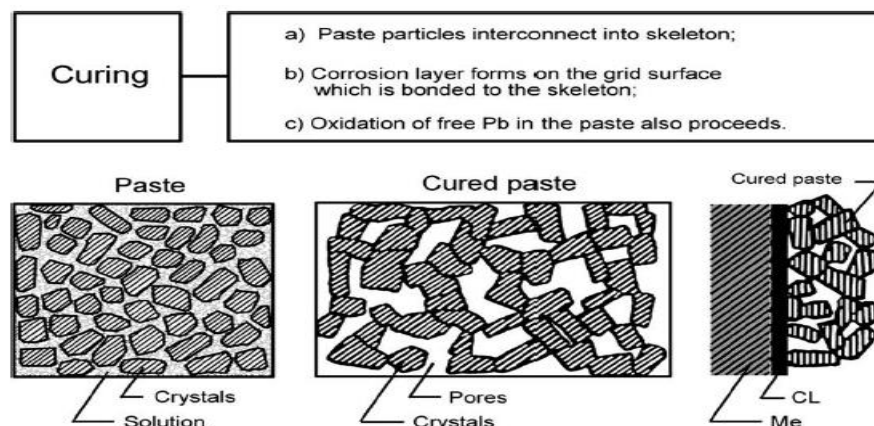
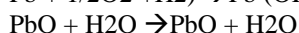
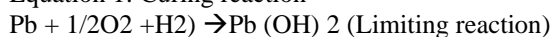


Figure 1: Pictorial explanation of the Curing process in Active material: Curing of Battery Plates, Pavlov DI [4]

Equation 1: Curing reaction



Concerning the application of 3BS crystals in cured plates for automotive batteries, while suitable for minimal depth of discharge scenarios, it falls short for higher depth of discharge applications. Curing performance hinges on several factors before delving into different profiles.

Factors affecting Chamber performance:

Chamber preparation and maintenance were evidently critical for consistent curing performance. Manufacturers employed two types of curing chambers: air - water mixing and steam - supplied processes. Aerosol supply curing chambers tended to exhibit higher inconsistency in process control, often due to difficulties in maintaining water pressure and nozzle blockages caused by foreign matter in the water supply. Predicting nozzle failure became challenging.

Aerosol - type curing chambers offered cost - effectiveness and yielded cured plate surfaces with minimal cracking. Conversely, steam - supplied chambers required higher investment and maintenance levels. Steam supply chambers provided consistent process control, lending themselves well to continuous production and higher temperature curing profiles. They maintained the required humidity levels to prevent sudden moisture loss from the plates. Therefore, for our curing temperature study, we opted for steam supply curing chambers.

Factors Affecting Paste Mixing Process:

Paste mixing plays a pivotal role in the curing process, necessitating the preservation of maximum residual lead levels and moisture content. Inadequate paste mixing methodologies can undermine curing reaction performance. The paste mixing sequence is as follows:



Figure 2: Paste mixing sequence.

Maintaining peak temperature during paste mixing was crucial, as it determined the formation of 3BS and 4BS crystals during curing [5]. To achieve this, paste mixing involved water cooling and air cooling. Battery manufacturers typically aim to sustain a prior mix temperature of 55 to 60°C by adjusting the acid flow rate with cooling assistance. Initially, the paste consisted of 3BS, which was later converted to 4BS during higher temperature curing profiles.

Tribasic sulfate pastes exhibited superior pastability compared to 4BS pastes, which were the result of aggressive acid addition and often exhibited poor pastability. Some manufacturers are employed.

The critical requirement for Oxide Mill production:

Attaining a favourable exothermic reaction in the curing process relied on the initial residual lead content of the oxide

mill. The standard specification for residual lead ranged from 28 - 32%, regardless of the oxide source. We had opted for ball mill oxide for plate manufacturing due to its high acid absorption properties. Lower residual lead content, below 15%, resulting from ageing, paste mixing, or pasting, was inadequate for effective curing reaction and could lead to poor bonding. We maintained a residual lead range of 20 - 25% after the pasting process [6].

Factors Affecting Pasting Process:

Following paste mixing, the paste was transferred to the pasting hopper and then applied to the grids. A flash drying oven was employed to maintain paste temperature above 50°C, initiating the curing reaction before loading into the chamber to prevent plate adhesion on the skid. Delays in pasting could lead to moisture loss. Consequently, a delay in the oxidation of residual lead resulted in plates with high residual lead content. For positive plates, free lead levels had to remain below 2%, and for negative plates, below 5%. High free lead content in the paste could hinder the conversion of

PbO₂, as 540Ah/Kg was required for free lead to convert into PbO₂ [7].

Enhancing moisture levels also involved monitoring and maintaining the pasting belt's longevity. We utilized a cotton belt paste machine for plate production, aiming to maintain high squeeze tension in the belt to enhance moisture absorption from the plate, thereby reducing internal moisture. Moisture analysis was conducted before and after the pasting process. Furthermore, meticulous belt maintenance was vital to prevent sulfate deposition, which could obstruct the belt's function. During idle periods, the belt surface was scrubbed with a copper wire brush and stored in water for the next setup. We maintained belt life by changing the belt for every 800, 000 plate productions. Figure 2 below represents the monitoring of belt life and the variation in plate weight for effective process control.

Belt Life Monitoring Graph:

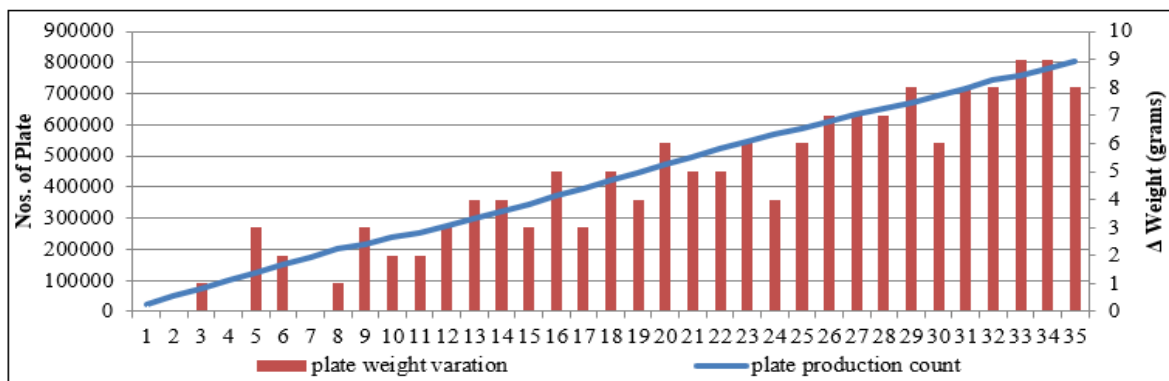


Figure 3: Represent the monitoring of belt life and the variation in plate weight.

The paste plates, released from the hopper, are then conveyed into the oven. Consequently, temperature and chain speed become critical factors. Before the curing process, the recommended moisture content after flash drying should be maintained at more than or equal to 8.5% for effective curing.

Experiment Description:

In that experiment, positive and negative plates were prepared using a common procedure. The positive plates underwent two different curing profiles: LTCP and HTCP. The curing profile for the negative plates remained unchanged. After production, the plates were extensively analysed using chemical and XRD methods. Once assembled, batteries were created using both LTCP plates and HTCP plates, with common negative plates. The batteries underwent formation in an acid circulation system, followed by a gel circulation process and gel conditioning charging.

Positive Plate Preparation:

Positive plates were manufactured using 1000 kgs of grey oxide from a ball mill, 12% of DM water, 8.33% of pure sulfuric acid leady oxide, and 2% of fiber. The peak temperature was set at 55°C, and acid addition was controlled to maintain the mixture temperature [7]. According to the peak temperature setting, Pb - Ca grids were used for pasting.

Curing Profiles:

Table 1: Low - temperature profile

Loading	45°C	95%	8 hours
Curing	45°C	95%	6.5 hours
Curing	55°C	95%	24 hours
Drying	60°C	0%	17.5 hours

Table 2: High - temperature profile

Loading	60°C	95%	8 hours
Curing	75°C	90%	20 hours
Drying	60°C	0%	12 hours

Negative Plate Preparation:

Negative plates were produced using 1000 kgs of grey oxide from a ball mill with 13.5% additives, including barium sulfate, Vanisperse - A, and carbon black, along with 10% water and 4.65% Pure sulfuric acid of Leady oxide. Pb - Ca grids were used for pasting [7], and the plate temperature was set at 55°C.

Table 3: Pasted plate analysis of both HTCP and LTCP:

Parameter	High Temperature Curing	Low Temperature Curing
Oxide Free Lead	30.8%	30.8%
Paste Density	4.05 gm/cc	4.05 gm/cc
Moisture	14.11%	14.11%
Paste Free Lead	26.5%	26.5%
Free Lead After Curing	1.5%	1.9%
After Curing Moisture	1.3%	1.2%

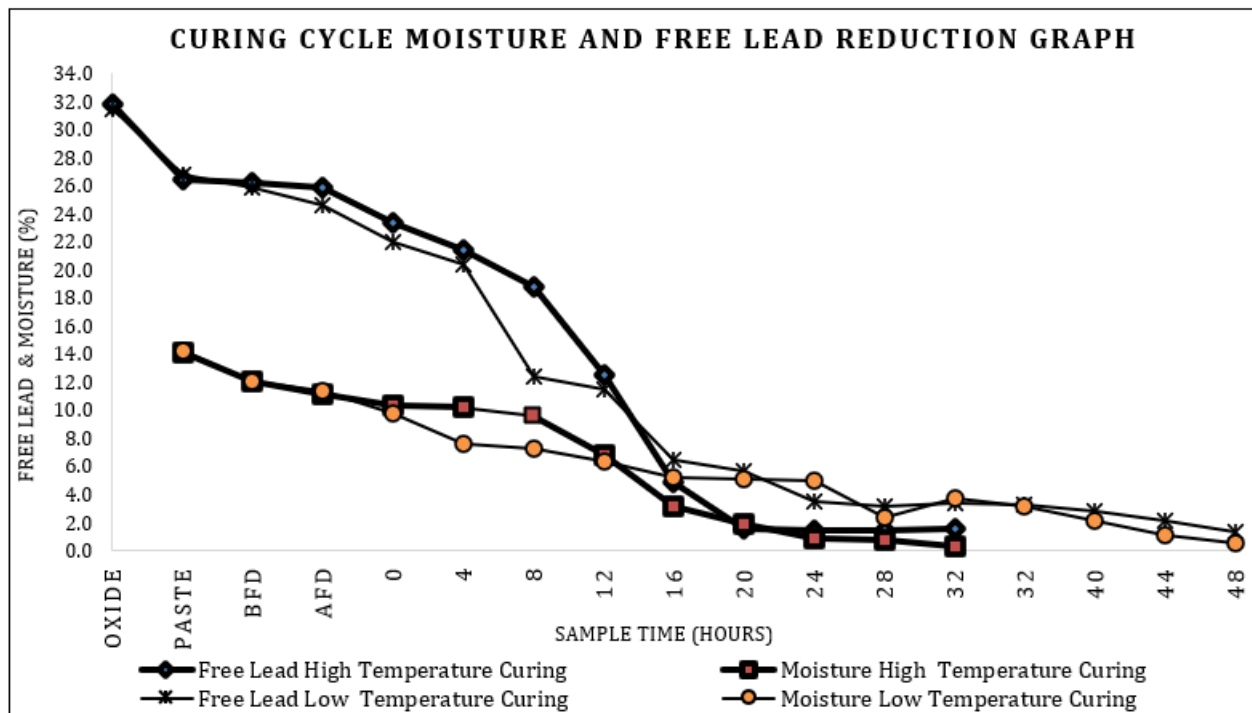


Figure 4: Curing Cycle Moisture and Free Lead Reduction Graph

Procedure for XRD and SEM

A spatula was used to remove the pasted active materials from the middle and from the corner of the cured plates into the sample holder [8]. XRD test was initiated using the Malvern Panalytical analytics machine.

Table 4: Material Characterization of XRD

Parameters	High Temperature Positive Curing	Low Temperature Positive Curing	Negative Curing
Lead Pb	0.55%	0.00%	0.39%
Tetragonal PbO	10.35%	46.90%	55.22%
Orthorhombic PbO	15.86%	1.62%	1.05%
1BS PbO. PbSo4. H2O	1.15%	1.69%	0.40%
3BS 3Pbo. PbSo4. H2O	6.37%	27.41%	39.90%
4BS 4Pbo. PbSo4. H2O	64.32%	15.84%	0.00%

In the table above and the XRD report below, it was evident that the HTCP plates had a higher 4BS content compared to the LTCP plates.

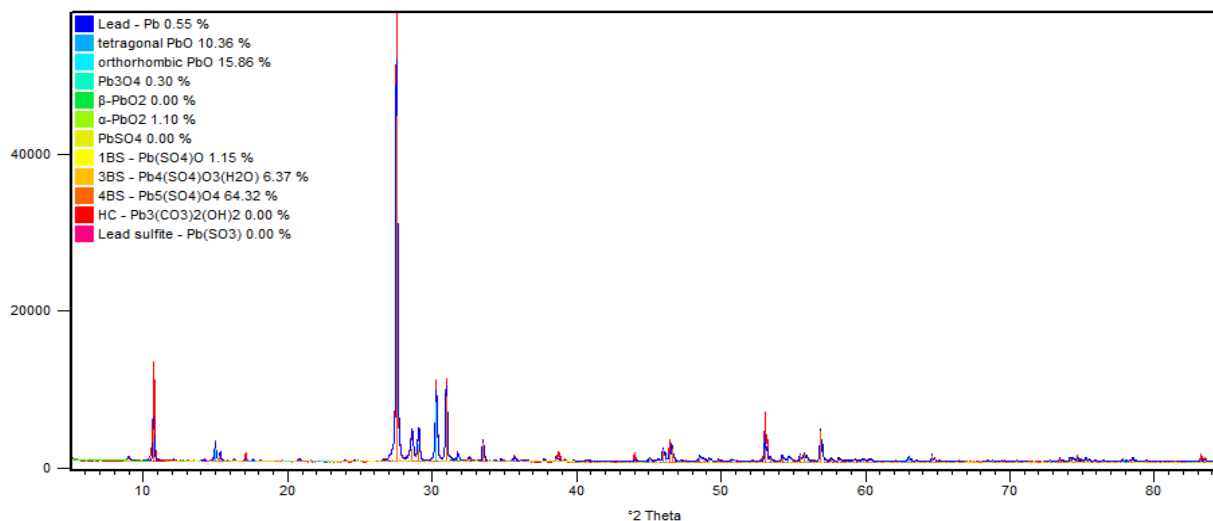


Figure 5: XRD report high temperature cured plate – Malvern Panalytical

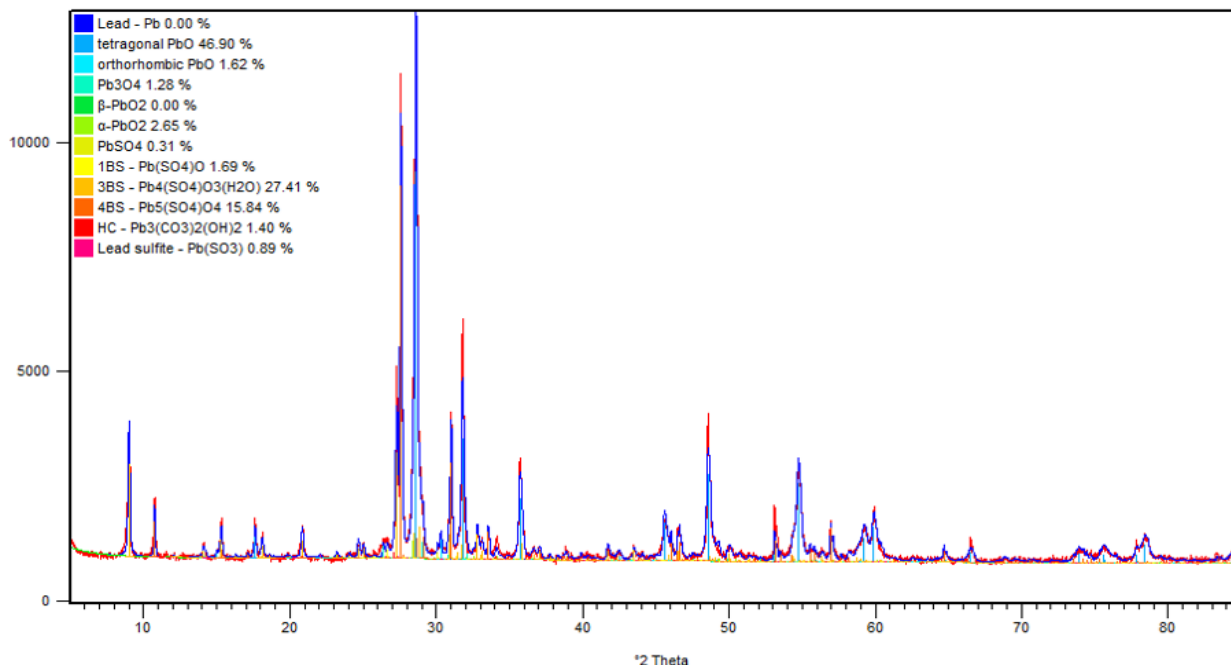


Figure 6: XRD report low temperature cured plate – Malvern Panalytical

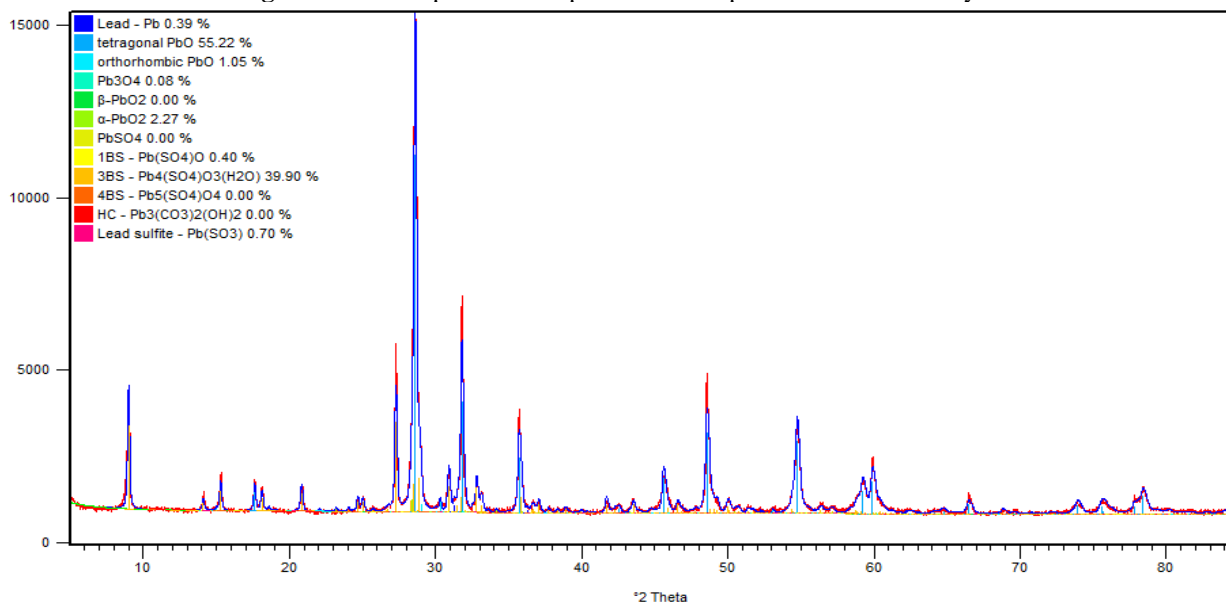


Figure 7: XRD report negative cured plate – Malvern Panalytical

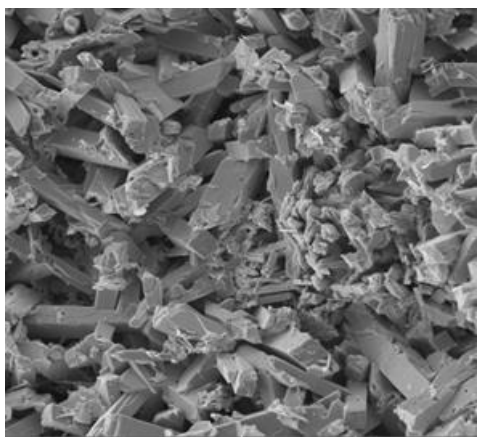


Figure 8: SEM report high temperature cured plate

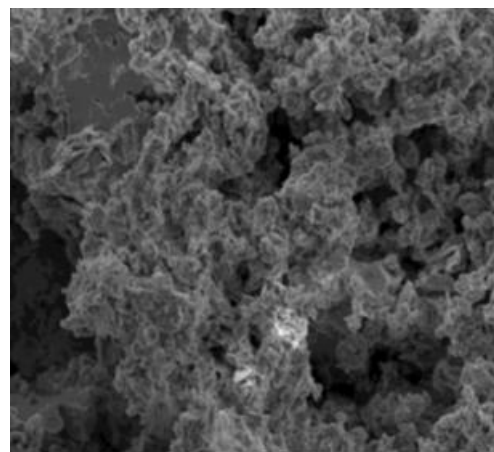


Figure 9: SEM report low temperature cured plate

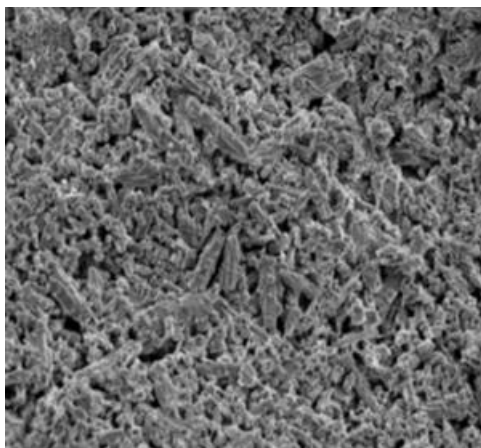


Figure 10: SEM report negative cured plate

SEM results were obtained from Black Diamond Structure’s R&D Lab. We sent our samples to them, and they tested them according to our requirements, providing us with the results. In the SEM images, it was evident that HTCP plates had a clear crystal structure due to having more 4BS crystals than LTCP plates [9].

Corrosion layer comparisons of the cured plate:

In the manufacturing process, we could not send all samples for SEM analysis to third parties because it would have taken

more time to get results. Therefore, we introduced a corrosion layer thickness procedure to evaluate the curing performance of the negative and positive plates. This was an internal procedure and did not require any cost.

Procedure:

We had taken a dry - cured plate and removed the paste from it. We used a soft brush to clean it thoroughly, ensuring no hard particles were left on the grid wires before recording its first weight as “W1”. We then boiled it in a hot 10% ammonium acetate solution, followed by rinsing and drying it at 80°C, and recorded the second weight “W2” after cooling. Afterwards, we immersed and boiled it in a 10% acetic acid solution, rinsed it, dried it at 80°C, and recorded the third weight “W3” after cooling.

Equation 2: Corrosion layer thickness

$$\text{Corrosion Layer thickness (micron)} = \frac{W2 - W3(g) * 10000}{\text{Density of the grid material}(g/cm^3) * \text{Grid area}(cm^2)}$$

Note:

*Grid area should be taken from AutoCAD data for accurate analysis.

This was the internal procedure used to measure the effectiveness of the curing for the continuous monitoring of the curing to maintain the process consistency.

Table 5: Comparison of the corrosion layer thickness of cured plate and visual comparisons:

Type	Results	Picture
High Temperature Curing	7 – 8 μm	
Low Temperature Curing	4 – 5 μm	

Porosity test:

After taking the dry - cured plate, we noted down its initial weight as “A”. Then, we immersed the plate in water for 12 hours and measured its weight as “B” while it was in the water. After taking it out and letting it drip dry for ten minutes, we weighed it again as weight “C” in the air. After that, we removed the material from the grid, dried the grid in the oven, and weighed it as weight “D”. Based on the above weights, we calculated Plate Volume “(C - B)”, Mass Weight “(A - D)”, Grid Volume (“D” /Alloy Density), Pore Volume “(C - A)”, and mass volume (plate volume - mass volume) [5].

Equation 3: Porosity

$$\text{Porosity} = \frac{\text{Pore Volume}}{\text{Mass Volume}}$$

RL%:

Took a dry - cured plate and removed the paste from it. Then, used a grinder to grind the paste and took a 10 - gram sample “W1” from it. This sample was immersed in a solution consisting of 30% ammonium acetate and 30% acetic acid with a volume of 100ml. After boiling it for 10 minutes, rinsed it thoroughly, washed it with acetone, and dried it at 120°C and measured the second weight as “W2”.

Equation 4: RL (%)

$$RL (\%) = \frac{W2 * 100}{W1}$$

Moisture:

Took a dry - cured plate and removed the paste from it. Removed 10 grams of dried paste from it and kept it inside the Moisture Analyzer at 120°C. After closing the drying chamber, the drying process starts automatically and calculating the moisture percentage.

Table 6: Corrosion layer thickness, porosity, RL, and moisture were tabulated below

Parameters	High - temperature cured positive plate	Low temperature cured positive plate	Standard Negative Cured plate
Corrosion layer thickness (Micron)	7 - 8	4 - 5	4 - 5
Porosity %	51	45	42
RL%	1.3	2.4	2.9
Moisture %	0.18	0.31	0.67

Assembly of batteries:

Batteries were assembled with 4 positive and 5 negative plates in each cell. Batteries were made with low - temperature - cured positive plates and high - temperature - cured plates. The negative plate was common for both trials.

Charging of batteries:

All batteries are formed with an acid circulation system formation module. The initial gravity of the acid was 1.110g/cc at 25°C temperature. After the soaking, it was allowed for 2 hours, during which the acid temperature was maintained using the cooling tower to avoid high temperatures and keep the cell temperature between 40 - 50°C. In the acid circulation system, each cell was connected by a nozzle with a filling hole and a suction hole. Filling of the acid took 15 - 20 minutes, respective of the volume of the batteries, and for the rest of the time, the acid was continuously circulated, filling the cell while simultaneously drawing hot acid through the suction hole [10]. This hot acid was sent to the cooling tower, then returned to the filling pipe after cooling and circulated through the filling hole at the nozzle. The batteries were kept with a 50mm gap to avoid high temperatures in the cell acid.



Table 7: Charging profile

Step	Current Density (mA/Cm2)	Hours (h)	Input Ah/Kg of Dry paste
1	6	2.00	26
2	12	2.00	52
3	18	3.00	111
4	21	3.50	156
5	12	2.00	52
6	21	0.50	22
7	21	1.25	56
8	12	2.00	52
9	26	0.75	42
10	21	1.25	56
11	12	2.00	52
Total		20.25	547

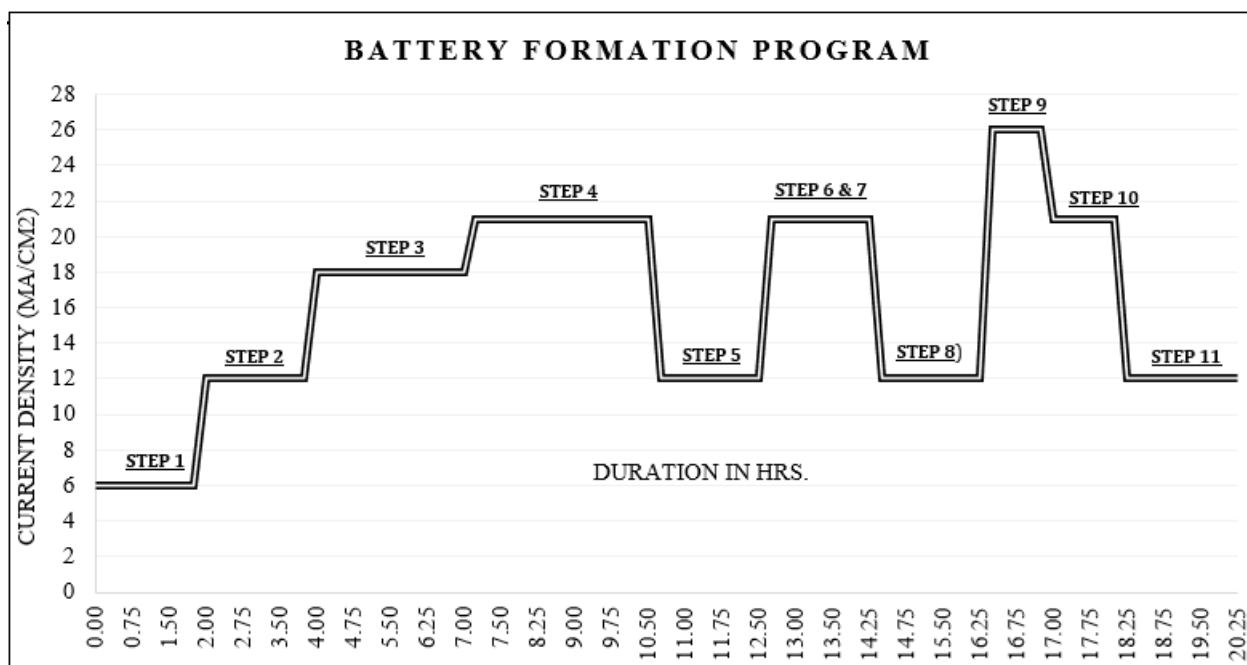


Figure 11: Battery Formation Program Time Vs Current Density

In the acid density system, the acid density slowly increased from 1.180 g/cm³ density of acid from step no 1 to step no 10. During the 11th step of charging, cells were adjusted to a final density of acid 1.300 g/cm³ by automatic switch - point

control, which controlled the raw acid and DM water dilution through a digital density meter for real - time data recording. Density and temperature graphs were recorded for the formation process on the computer for our reference.

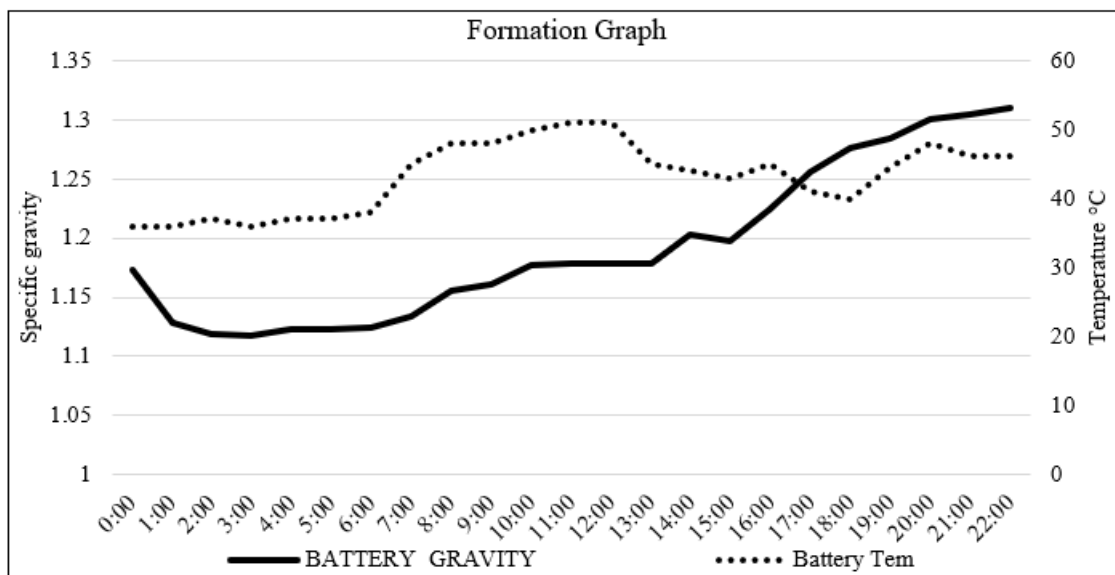


Figure 12: Formation graph Specific gravity and temperature vs. Time

After formation, we checked the acid density of each cell. Once the gravity reached 1.300g/cm³, those batteries were discharged at a C5 rating in the formation without acid circulation. The discharge criteria were fixed at 10.2V and 1.130±0.005 gm/cm³. Once all batteries reached 1.130g/cm³ density, then the circuit was disconnected by the auto mode commands. Then, all the batteries' acid was exchanged by 6% fumed silica and 1.130g/cm³ acid in a gel mixing and exchange machine. In this process, each battery was connected by nozzles, which had filling and suction holes. The prepared 6% silica gel acid mixture was pumped from the gel mixing tank and supplied through the filling hole of the nozzle. The liquid acid was sucked by the suction hole and then reached the gel mixing tank. This exchange process took 2 hours. After gel circulation, silica samples were taken from the cells randomly, and the chemical composition was

checked and confirmed. During this gel circulation, the silica - mixed acid temperature was maintained below 10°C. These batteries stand for 24 hours at the ambient temperature, equal to room temperature.

Once the environmental temperature was reached, all batteries were connected to the rectifier for the refresh gel conditioning charging. The charging input is given at 1.25 times the discharged AH. At the end of charging, the gel became hard. The trial batteries were sent for capacity and 70% DoD cycling.

Electrical Test:

We tested both batteries following the guidelines outlined in IEC 60254 - 1 for a 70% Depth of Discharge (DOD).

Table 8: Battery details

Parameters	Specification	Remark
Battery type	BCI - 34	54Ah[at]5 hours
Plate Coupling	Positive Plate – 4 Nos. Negative Plate – 5 Nos.	
Container	Dimensions: Length: 254 mm, Width: 168 mm, Height: 175 mm.	Plastic Material: ABS
Nominal Voltage	12V	Cut off Voltage during discharge - 10.2V
Open Circuit Voltage	Full Charge - 13.30V	At cut - off Voltage - 10.2V

Procedure:

- a) Discharge the battery for 3.5 hours at a current of I (A) = 0.2C.
- b) Recharge it for a maximum of 14 hours immediately after the discharge, maintaining a constant voltage not exceeding 2.35V per cell. During the last 2 hours of the recharge, ensure that the current does not exceed I (A) = CN (Ah) / 66.66 (h).

The tested battery is rated at CN = 54Ah, and the discharge current is set at 10.8Amps. According to the standard, we initiated the battery discharge at 10.8A for 3.5 hours. After every 49 cycles, we conducted a capacity test. If the capacity falls below 80%, we terminate the battery testing.

The high - temperature - cured battery performed well in the electrical test results, achieving more than 620 cycles. However, the low - temperature - cured battery exhibited poor

performance, reaching only 200 cycles and falling below 80% capacity.

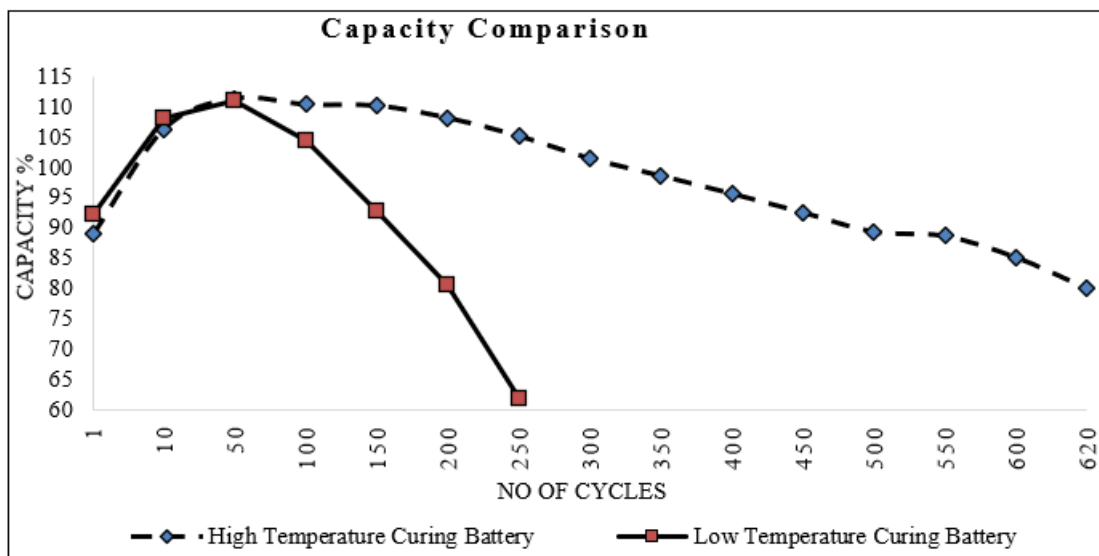


Figure 13: Cycle life capacity comparison

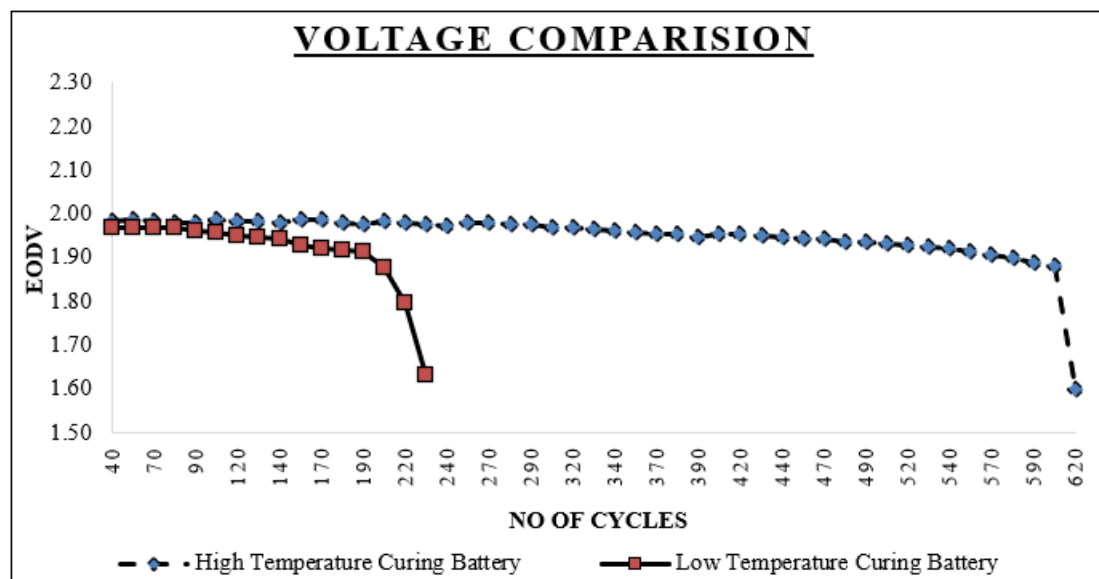


Figure 14: Cycle life voltage comparison

Formed plate analysis:

solution and continue titrating until the blue color disappeared.

PbO2 Analysis:

After neutralizing the formed plate in DM water, dry it at 60°C and ground it. After that, the sample was passed through a 150 μ sieve. Took 0.5gm of sample into 500 conical beakers, then added 60ml of dissolving solution (30% Acetic Acid and 30% Ammonium acetate solution) and 10ml of KI solution with continuous stirring; immediately start the titration process using 0.1M sodium thiosulphate solution until a pale - yellow color emerges, then introduce 1ml of starch indicator

Equation 5: % PbO2 in sample

$$\% \text{ PbO}_2 \text{ in sample} = \frac{1.196 \times \text{mili liters of Sodium thiosulphate}}{\text{Sample weight (g)}}$$

Positive plates were washed with DM water until the pH of the plate turned to 6 to 7. The plate was dried at 60°C for 12 hours and was sent for XRD and SEM analysis. The results are tabulated in the table.

Table 9: Material characterization analysis

Parameters	HIGH TEMPERATURE CURED POSITIVE FORMED PLATE	LOW TEMPERATURE CURED POSITIVE FORMED PLATE
Lead Pb (%)	0.82	0.34
Tetragonal PbO (%)	1.33	2.30

Orthorhombic PbO (%)	0.42	1.02
Minium Pb3O4 (%)	2.67	2.71
Plattnerite PbO2 (%)	80.12	62.19
Scrutinyite PbO2 (%)	6.12	24.51
Anglesite PbSO4 (%)	5.82	2.01
Lanarkite Pb (SO4) 0	0.62	0.62
3BS - Pb4 (SO4) O3 (H2O)	2.04	1.95
4BS - Pb5 (SO4) O4	0.16	2.35

XRD and SEM result [8], [9]:

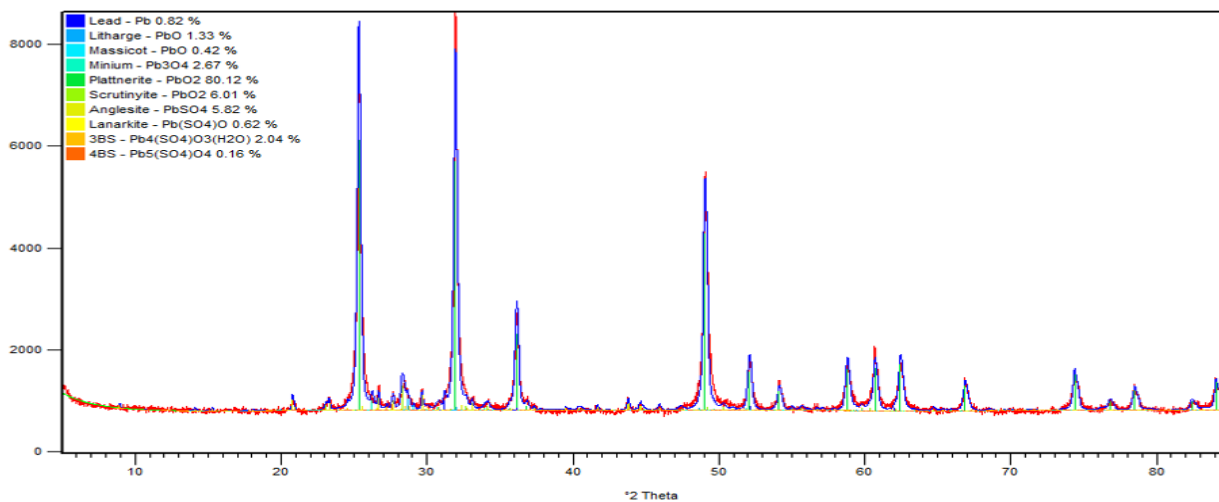


Figure 15: XRD report high temperature formed plate

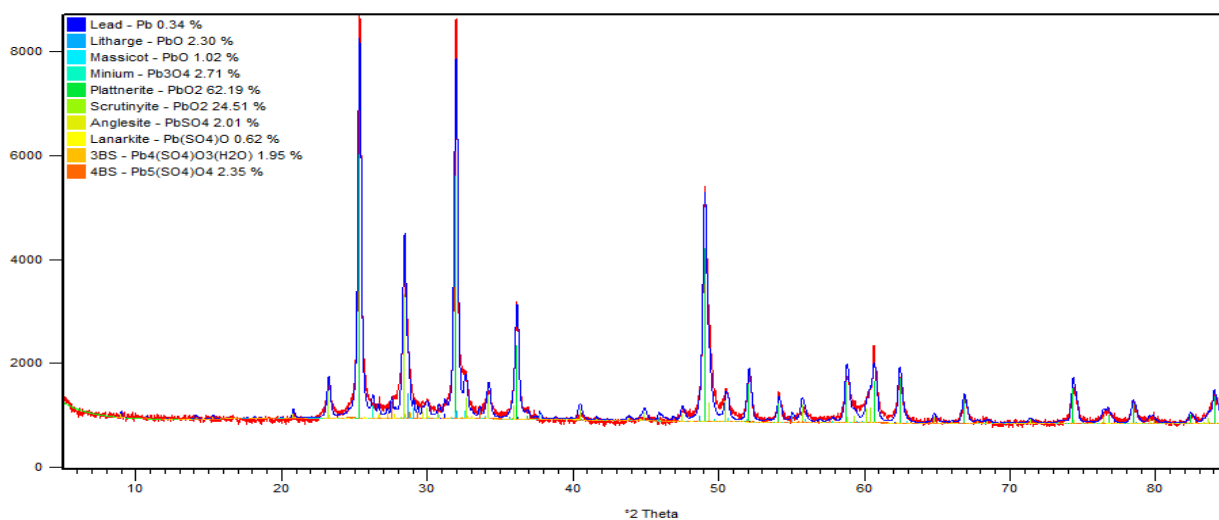


Figure 16: XRD report low temperature formed plate

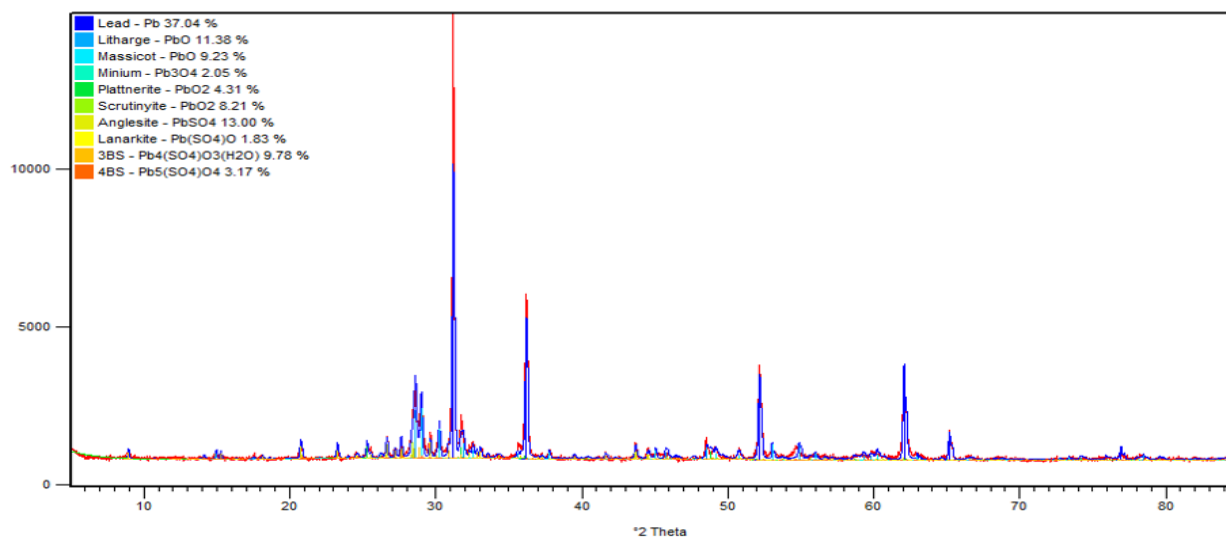


Figure 17: XRD reports negative formed plate

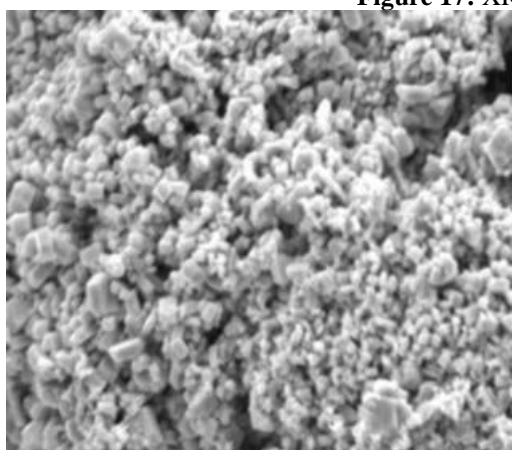


Figure 18: SEM report high temperature formed Positive plate

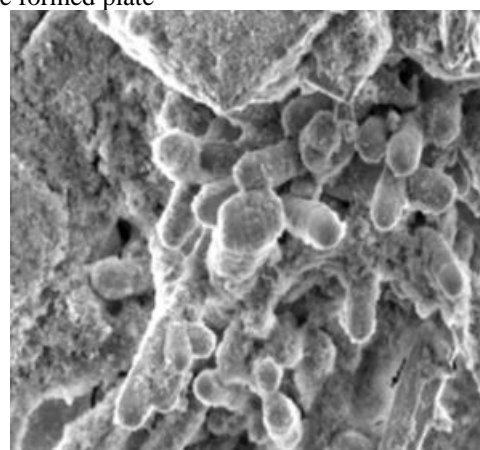


Figure 20: SEM report negative formed plate

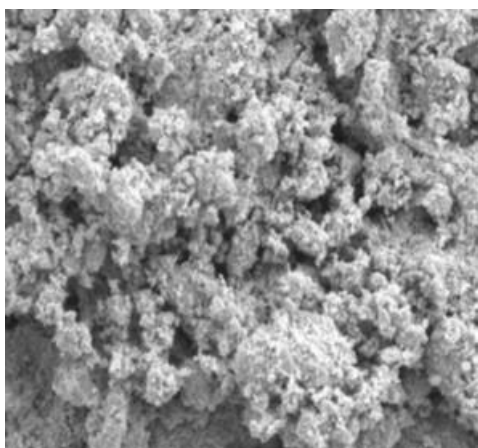


Figure 19: SEM report low temperature formed Positive plate

2. Result and Discussion

The cured negative plate XRD analysis showed the predominant phase of 3BS, as shown in the picture graph. The low - temperature cured positive plate predominant phase was 3BS, and that high - temperature cured positive plate was 4BS and PbO₂ of the plate.

SEM;

The SEM analysis on the cured plate showed a uniform 3BS crystal structure with 2 to 3 microns [9]. The low - temperature cured positive plate showed a uniform 3BS crystal size of 5 to 10 microns, and the high - temperature cured positive plate showed a uniform crystal size of 30 to 40 microns. Uniform PbO₂ crystal in the positive plate.

3. Conclusion

Based on the result of this study, the following result can be excluded with respect to the different curing algorithms of the positive plate. Physical characteristics of the low - temperature positive plate show the uniform crystal structure in the formed plate. The physical characteristics of the high - temperature cured plate show the uniform crystal structure on the formed plate. 70% DOD for the low - temperature cured positive plate used a battery given 200 cycles, and the high - temperature cured plate used a battery given 620 cycles. This study highlighted the significant impact of the curing

temperature algorithm on the life cycle performance of gelled valved regulated lead acid batteries. The high - temperature curing profile (HTCP) resulted in high corrosion layers, improved adhesion and cohesion, and enhanced cycling performance when compared to the low - temperature curing profile (LTCP). Manufacturers could optimize the curing process by adopting a higher temperature curing Algorithm, which could lead to improved battery cycle life. This research provided valuable insights for the lead acid battery industry, contributing to the development of the most effective and durable gelled valve - regulated lead acid batteries.

Acknowledgements:

The authors wish to express their gratitude to the Eternity Technologies Chemical Lab for providing the necessary research infrastructure and testing facilities for this study. Additionally, we thank Black Diamond Structure TM for supplying the SEM analysis report for our research paper.

Funding Information:

This research was conducted as part of Eternity Technologies FZ - LLC company's research and development efforts and did not receive funding from external agencies.

References

- [1] R. Wagner and M. Accu, "Curing and Formation."
- [2] B. Sundén, "Applications of batteries, " in Hydrogen, Batteries and Fuel Cells, Elsevier, 2019, pp.111–122. doi: 10.1016/b978 - 0 - 12 - 816950 - 6.00007 - 5.
- [3] Time Reduction of Deep Cycle Lead Acid Battery Negative Plate Curing Process by Changing Curing Parameters.2019.
- [4] D. Pavlov, "Curing of Battery Plates, " in Lead - Acid Batteries: Science and Technology, Elsevier, 2011, pp.363–404. doi: 10.1016/B978 - 0 - 444 - 52882 - 7.10008 - 4.
- [5] Detchko Pavlov, Lead - Acid Batteries: Science and Technology.2011.
- [6] M. G. Mayer and D. A. J. Rand, "Lead oxide for lead/acid battery positive plates: scope for improvement?," 1996.
- [7] D. Pavlov, "Additives to the Pastes for Positive and Negative Battery Plates, " in Lead - Acid Batteries: Science and Technology, Elsevier, 2017, pp.335–379. doi: 10.1016/b978 - 0 - 444 - 59552 - 2.00007 - 9.
- [8] T. U. Schulli and S. J. Leake, "X - ray nanobeam diffraction imaging of materials, " Current Opinion in Solid State and Materials Science, vol.22, no.5. Elsevier Ltd, pp.188–201, Oct.01, 2018. doi: 10.1016/j.cossms.2018.09.003.
- [9] M. De, A. Pereira - Da - Silva, and F. A. Ferri, "1 - Scanning Electron Microscopy, " 2017. doi: 10.1016/B978 - 0 - 323 - 49778 - 7/00001 - 1.
- [10] M. A. Kashem, A. Fattah, S. M. S. Farhan, and N. Nafis, "Fast Formation of Tubular Plate Deep Cycle Lead Acid Battery by Acid Recirculation System (ACS), " in Fast Formation of Tubular Plate Deep Cycle Lead Acid Battery by Acid Recirculation System (ACS), IEEE, Feb.2019, pp.1–6. doi: 10.1109/ECACE.2019.8679320.